

**Dieses Dokument ist eine Zweitveröffentlichung (Verlagsversion) /
This is a self-archiving document (published version):**

Judith Hahner, Claudia Hinüber, Annette Breier, Tobias Siebert, Harald Brünig, Gert Heinrich

Adjusting the mechanical behavior of embroidered scaffolds to lapin anterior cruciate ligaments by varying the thread materials

Erstveröffentlichung in / First published in:

Textile Research Journal. 2015, 85(14), S. 1431 – 1444 [Zugriff am: 07.08.2019]. SAGE journals. ISSN 1746-7748.

DOI: <https://doi.org/10.1177/0040517514566107>

Diese Version ist verfügbar / This version is available on:

<https://nbn-resolving.org/urn:nbn:de:bsz:14-qucosa2-354017>

„Dieser Beitrag ist mit Zustimmung des Rechteinhabers aufgrund einer (DFGgeförderten) Allianz- bzw. Nationallizenz frei zugänglich.“

This publication is openly accessible with the permission of the copyright owner. The permission is granted within a nationwide license, supported by the German Research Foundation (abbr. in German DFG).

www.nationallizenzen.de/

Adjusting the mechanical behavior of embroidered scaffolds to lapin anterior cruciate ligaments by varying the thread materials

Textile Research Journal
2015, Vol. 85(14) 1431–1444
© The Author(s) 2015
Reprints and permissions:
sagepub.co.uk/journalsPermissions.nav
DOI: 10.1177/0040517514566107
trj.sagepub.com


Judith Hahner^{1,2}, Claudia Hinüber^{1,2}, Annette Breier²,
Tobias Siebert³, Harald Brünig² and Gert Heinrich^{1,2}

Abstract

Traumatic rupture of the anterior cruciate ligament (ACL) can cause local destabilization and loss of mobility. Reconstruction using engineered ACL grafts is rarely successful due to sub-optimal material choice and mechanical performance.

Thus, the presented work demonstrates the fabrication of various embroidered single- and bi-component scaffolds made of two commercially available monofilament threads (polydioxanone, poly(lactic acid-co- ϵ - caprolactone)) as well as a novel melt spun poly(L-lactic acid) multifilament and their mechanical analysis by tensile tests and under cyclic loading. Selected scaffolds, adjusted by material composition and textile parameters, revealed a load–strain behavior comparable to native lapin ACL tissue exhibiting a sufficient amount of elastic deformation within the toe-region of 1.7%, scaffold stiffness of 123 N/mm and adequate maximum tensile load (300 N) and strain (20%). Therefore, the design of resorbable embroidered bi-component scaffolds represents a promising approach to replace artificial non-resorbable ligament grafts and allows for innovative tissue engineering strategies.

Keywords

embroidery technology, mechanical properties, ACL, rabbit, structure properties, scaffold, medical textiles

Forty percent of all clinical common knee injuries are related to the lesion of ligaments.¹ Among these injuries rupture of the anterior cruciate ligament (ACL), appearing due to rotary motion of the knee joint with fixed lower leg,^{2,3} is the most frequent ligament injury (47%) and results in dynamic destabilization and loss of mobility.^{4–6}

Conventional reconstructions are made of autologous tissue of the patellar and semitendinosus tendon.^{6,7} Disadvantages such as the limited availability, the high morbidity rate and a deviant mechanical behavior^{8,9} lead to the introduction of non-resorbable synthetic grafts, such as the Leeds-Keio prosthesis. However, high failure rates due to material abrasion and fatigue strictly limit their application.^{10,11}

As a new research field, tissue engineering initializes innovative strategies for ligament tissue reconstruction.^{9,12,13} To address the demands of clinical practice,

we aim to develop a triphasic embroidered scaffold from resorbable polymers, temporarily mimicking native ACL structure and function until regeneration has been completed.

In particular, textile technologies offer the possibility to fabricate variable mechanically stable structures used as scaffolds for temporary ACL replacement. Scaffold properties, such as viscoelastic behavior, mechanical

¹Technische Universität Dresden, Institute of Materials Science, Germany

²Leibniz-Institut für Polymerforschung Dresden e. V., Germany

³University of Stuttgart, Institute of Sport- and Movement Science, Germany

Corresponding author:

Judith Hahner, Leibniz-Institut für Polymerforschung Dresden e. V., Hohe Straße 6, D-01069 Dresden, Germany.
Email: hahner@ipfdd.de

anisotropy or porosity, can be tailored by the material composition and the textile parameters.^{14,15} Braiding as a textile technology for ligament reconstruction creates tubular structures with adjustable mechanical properties and a variable scaffold morphology, which are determined by the used braiding angle, the thread material and fiber diameter.^{16–20} Freeman et al.¹⁸ designed a poly(L-lactic acid) (PLA) braid-twist scaffold exhibiting a maximum tensile load of about 300 N (81.6 MPa for a cross-sectional area of 3.7 mm²) and a yield point of ~80 N. Walters et al.²⁰ studied braid-twist scaffolds made of cross-linked collagen fibers. The collagen scaffolds demonstrated an averaged maximum tensile load of 7.92 N and a stiffness of 2.80 N/mm. Sahoo et al.²¹ investigated different one-dimensional scaffolds made of knitted and woven structures from poly(lactic acid-co-glycolide) (PLGA). The woven scaffolds showed a higher maximum tensile load (97.2 N) compared to knitted scaffolds (68.4 N). However, the braided, knitted or woven structures fabricated from collagen, PLA and PLGA showed insufficient mechanical properties for ACL reconstruction.

Compared to the above-mentioned textile processing methods, embroidery technology offers a wider range of design parameters to tailor the specific structural and mechanical properties of ACL.^{22,23} In order to mimic the mechanical behavior of ACL, thread materials can be arranged in location and orientation.²⁴ Structural gradients can be introduced by means of different patterns that are realized by variable stitch length and stitch angles.²⁵ Thus, embroidery technology allows for the fabrication of three-dimensional (3D) scaffolds with different structure zones. Due to the possibility of manufacturing in small batches custom-made embroidered textile implants can be designed efficiently and produced with low costs.²² Rentsch et al.²⁶ successfully performed an *in vivo* study applying embroidered bioactive, surface-coated poly(lactic acid-co- ϵ -caprolactone) (P(LA-CL)) scaffolds as bone implants in a tibia critical size defect model. Hoyer et al.²⁷ tested embroidered scaffolds made of P(LA-CL) and polydioxanone (PDS) with collagen supplementation for ligament tissue engineering. The results related to the cell adherence, cell vitality and extra-cellular matrix synthesis indicate that embroidered P(LA-CL) scaffolds functionalized with collagen foam may serve as a promising basis for ACL replacement.

Hence, a scaffold consisting of a resorbable embroidered structure could be a potential substrate for a regenerative approach as temporary replacement of ruptured ACL. The most crucial point is the imitation of the specific load-strain behavior of an ACL with characteristic mechanical parameters, such as toe-region and stiffness.^{3,28–30} Furthermore,

the typical viscoelastic behavior that native ligament tissue exhibits under cyclic loading needs to be adjusted for embroidered scaffolds.³¹ The aim of the study is the mechanical analysis of various embroidered single- and bi-component scaffolds made of two commercially available monofilament threads (PDS, P(LA-CL)) as well as a novel melt spun PLA multifilament by tensile tests and under cyclic loading. In addition, the viscoelastic behavior of native lapine ACL has been investigated in order to obtain control parameters for the mechanical analysis of the embroidered scaffolds and reference values for the purpose of comparison.

Material and methods

Sample preparation

Scaffolds. Textile scaffolds were fabricated by means of an embroidery machine (ZSK JCZ 0209-550, ZSK Stickmaschinen GmbH, Germany), as described elsewhere.²⁵ Therefore, commercially available suture threads (provided by Catgut GmbH, Germany) PDS (Samyang Biopharmaceuticals Corp., Korea) and poly(lactic acid-co- ϵ -caprolactone) (P(LA-CL), Gunze Ltd, Japan) were used. Both monofilaments were used in size USP 7-0 (United States Pharmacopeia), which corresponds to an averaged thread diameter of 85 μ m (100 dtex). In contrast to the monofilaments, PLA (polymer 6202D; NatureWorks LLC, USA) was melt spun at the Leibniz-Institut für Polymerforschung Dresden e. V. to a multifilament thread (single filament diameter 20 μ m, 12 filaments with 80 dtex) with a take-up velocity of 3000 m/min and a draw ratio of 1.6. Finally, the multifilament thread was twisted to a ply yarn (320 dtex, S 20 \times 2, Z 40 \times 2). Embroidered structures were manufactured with one upper thread and one lower thread. All above-mentioned thread materials were applied as upper and/or lower thread and all possible mono- or bi-component structures, for example PLA/PLA, PLA/PDS, PLA/P(LA-CL), PDS/PDS, PDS/PLA, etc., were fabricated and mechanically tested (see Appendix 1 for identification of upper and lower threads, for example P(LA-CL)-PDS). The ratio of the upper thread to the lower thread is 2:1. This ratio is determined by the embroidery technology and allows an optimal manufacturing process with a low number of thread breakages associated with a precise embroidered pattern. The process of embroidery enables the manufacturing of reproducible two-dimensional (2D) layers. Each layer exhibits a pattern with 1.8 mm stitch length, 15° stitch angle and 0.2 mm duplication shift (Figure 1). In preliminary tests the optimal pattern, which meets the required mechanical properties, was evaluated by means of statistical evaluation of

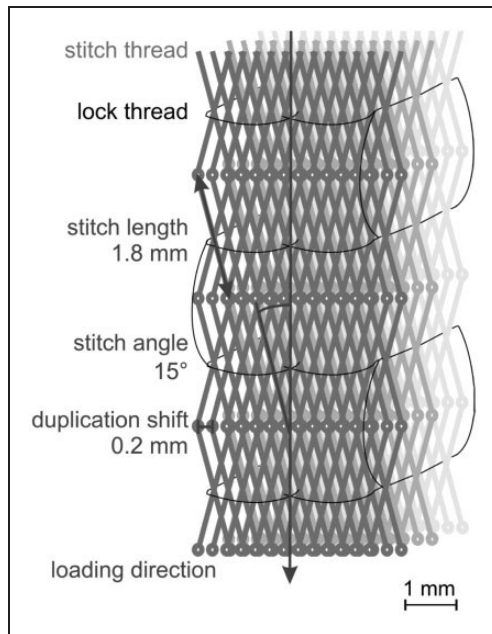


Figure 1. Embroidery pattern (defined stitch length, stitch angle and duplication shift) of the scaffold consisting of three layers stacked and locked.

patterns with varying stitch length, stitch angle and duplication shift (Appendices 2–4). In order to build up a 3D scaffold, three 2D layers were stacked one upon the other and locked by the use of a lock thread and a positioning device. The locking was performed with the same upper and/or lower thread materials as used for the 2D layers. Two-dimensional structures were embroidered on water soluble polyvinylalcohol (PVA) nonwoven substrate (Freudenberg Einlagestoffe KG, Germany), which was washed out subsequently after the locking procedure in water for 6 hours at ambient temperature. Three-dimensional scaffolds were fabricated with dimensions of 30 mm length, 4 mm width and 2 mm height according to the dimension of the lapin ACL.

Preparation of native lapin ACL tissue. Lapin knee joints were obtained from dead animals, which were used before in animal studies within veterinary science courses and in final experiments to examine the muscle properties of the calf muscles.³² These experiments were approved according to Section 8 of the German animal protection law (Tierschutzgesetz, BGBl. I 1972, 1277). No animals were killed especially for this study. The ACL were dissected free of knee joint tissue as the femur–tibia complex. Native ACL (Table 1) from female New Zealand White Rabbits of different age groups (number of juvenile ACL, $n=2$, weight ≤ 3000 g; number of adult ACL, $n=4$, weight > 3000 g) were prepared directly before testing

Table 1. Properties of the investigated native anterior cruciate ligament (ACL) of juvenile (ju) and adult (ad) rabbits

	Location	Animal weight [g]	Measures [mm] (length \times width \times height)
ACL-ju1	Left	3000	$9 \times 2.5 \times 4$
ACL-ju2	Right	2760	$9 \times 2 \times 4$
ACL-ad1	Left	4580	$9.5 \times 3 \times 4$
ACL-ad2	Left	5400	$8.5 \times 2 \times 4$
ACL-ad3	Right	4580	$10 \times 2 \times 4$
ACL-ad4	Right	5400	$10 \times 2 \times 3$

and kept moist with phosphate-buffered saline (PBS) at any time.

Femur and tibia were cut to a length of 30–40 mm (Figure 2). Subsequently, mechanical testing was carried out. ACL dimensions were determined at rest length using a caliper.

Mechanical testing

Cyclic tensile testing of ACLs. Cyclic tensile testing of ACL was performed by means of a muscle lever (310B-LR, Aurora Scientific Inc., Canada), which was successfully used in former studies to determine the viscoelastic properties of the lapin muscle–tendon complex.³² Preliminary tests indicated an amplitude of 1.8 mm at most (equates to 20% strain for 9 mm mean length of lapin ACL) as a reasonable test parameter. Amplitudes higher than 1.8 mm indicated the beginning of ligament damage (cracking). Physical performance tests were carried out with amplitudes of 1.6 and 1.8 mm and testing velocities of 5 and 20 mm/s, respectively. Five hysteresis loops of each test were recorded to determine the values for energy dissipation, stiffness and toe-region (see the *Mathematical and statistical analysis* section for explanatory notes). The ACL load was measured at a sample rate of 1000 Hz. The gauge lengths l_{gauge} of the tested ACLs were determined separately and varied between 8.5 and 10.0 mm (Table 1). Metal clamps were used for fixation of the femur–tibia complex. During testing ACLs were constantly kept moist with PBS.

Cyclic tensile testing of scaffolds. The test conditions for cyclic tests of the embroidered scaffolds were predefined based on the results of ACL testing. Therefore, a Zwick/Roell Z010 (Zwick/Roell, Germany) tensile testing machine with pneumatic metal clamps was used. The gauge length of the scaffolds was set to 10 mm. Hysteresis loops with 10% (equates to 1.0 mm amplitude) and 20% (equates to 2.0 mm amplitude) strain and 5 and 20 mm/s testing velocity were performed, respectively. Scaffolds (number of scaffolds, $n=3$)

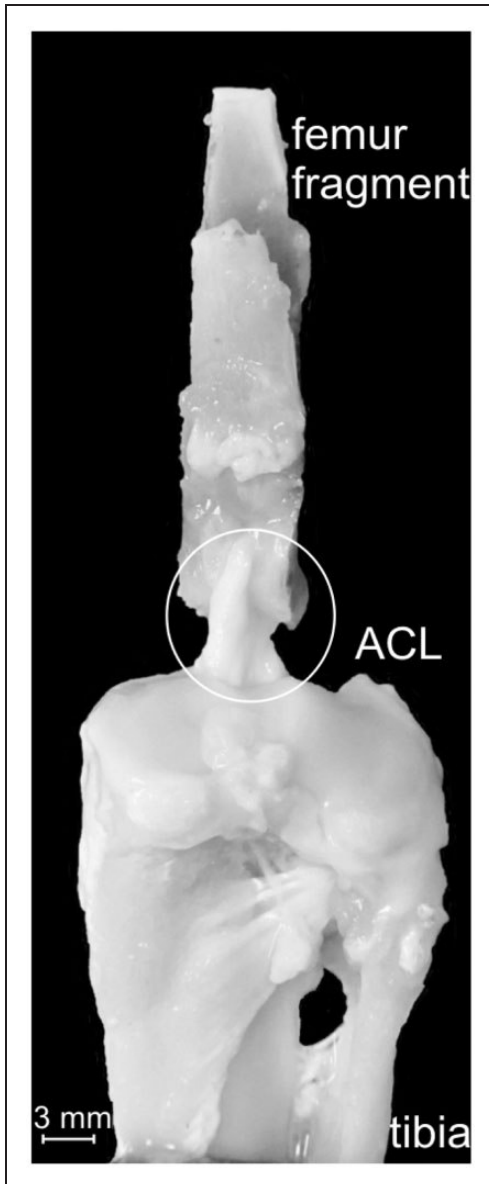


Figure 2. Lapin anterior cruciate ligament (ACL) prepared in the femur–ligament–tibia complex for cyclic tensile testing.

were tested in the dry state. The following test runs were conducted in series with each scaffold: (A) 10% strain and 5 mm/s testing velocity; (B) 20% and 5 mm/s; (C) 20% and 20 mm/s; and (D) 10% and 5 mm/s. Fixation was corrected after each run to ensure a constant gauge length. Test runs (A) and (D) were carried out using similar parameters in order to compare the mechanical properties of the embroidered scaffolds after different cyclic loadings. Energy dissipation values were determined (see the *Mathematical and statistical analysis* section for explanatory notes).

Uniaxial tensile testing of scaffolds. Tensile and strain properties of the unloaded (un) and the preloaded (by cyclic

tensile testing, pre) scaffolds ($n=3$) were studied by uniaxial tensile testing using a Zwick/Roell UPM 2.5 tensile testing machine (1000 N load sensor) controlled with TestXpert software (Zwick/Roell, Germany). The gauge length of the scaffolds was 10 mm. The test speed was 10 mm/s. Pneumatic metal clamps were used. The maximum tensile load, maximum strain, stiffness, yield load and toe-region were determined (see the *Mathematical and statistical analysis* section for explanatory notes).

Mathematical and statistical analysis

The measured data of lapine ACL was evaluated by averaging adjacent data points to decrease the noise of raw data. The number of averaged data points varied between five data points for a testing velocity of 20 mm/s and ten data points for a testing velocity of 5 mm/s. These averaged data sets were presented as load–displacement diagram.

The scheme in Figure 3(a) represents such a curve $F(l)$ and the first derivative $F'(l)$ of this function. The first derivative was qualitatively subdivided into three parts. The first plateau defines the toe-region D_{toe} [%] by Equation (1):

$$D_{toe} = \frac{l_{toe}}{l_{gauge}} \times 100\% \quad (1)$$

with the length ratio of the toe-region l_{toe} to the gauge length l_{gauge} . It is followed by an increasing parabolic part and ends with the second plateau that defines the stiffness S [N/mm] by Equation (2):

$$S = \frac{\Delta F}{\Delta l} \quad (2)$$

where ΔF is the applied load and Δl the displacement caused by the applied load. These mechanical parameters were determined by manual metering. Toe-regions were presented in percentages and referred to the length of each ACL (Table 1) and to the gauge length for embroidered scaffolds, respectively.

The maximum tensile load F_{max} [N] and maximum strain ε_{max} [%] were only determined for embroidered scaffolds by Equation (3):

$$\varepsilon_{max} = \frac{l_{max}}{l_{gauge}} \times 100\% \quad (3)$$

with the length ratio of maximum length l_{max} to gauge length l_{gauge} . The yield point (yield load and yield strain) of the embroidered scaffolds was defined as the point at which the slope of the curve turns to zero (Figure 3(a)) and the structure begins to deform plastically.

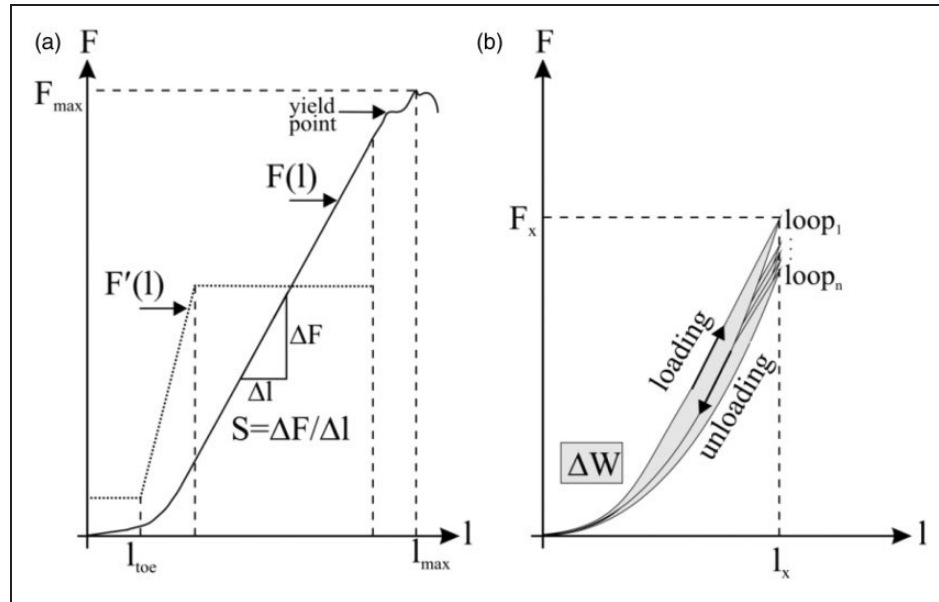


Figure 3. Scheme of a load–displacement diagram to define the mechanical parameters (a) maximum tensile load F_{max} , maximum strain ϵ_{max} ($\epsilon_{max} = (l_{max}/l_{gauge}) \times 100\%$), stiffness S , toe-region D_{toe} ($D_{toe} = (l_{toe}/l_{gauge}) \times 100\%$), yield point and (b) energy dissipation ΔW .

Energy dissipation ΔW [mJ] was averaged out of the area of the hysteresis loops for native ACL and embroidered scaffolds, respectively. The energy dissipation is defined in Equation (4) as

$$\Delta W = \frac{1}{n} \times \sum_{loop_1}^{loop_n} \left(\int_0^{l_x} F_{x,loading}(l_x) - F_{x,unloading}(l_x) dl \right) \quad (4)$$

where $loop_n$ is the number of hysteresis loops, F_x [N] is the load and l_x [mm] is the measured length (Figure 3(b)).

For statistical analysis of two unpaired groups, analysis of variance was performed as a two-sample Student's t -test ($p < \text{significance level}$: $*p < 0.05$, $**p < 0.005$). Results for mechanical properties were represented as a mean \pm standard deviation (mean \pm SD).

Results

Native lapin ACL

Averaged stiffness was determined to be (121.6 ± 12.2) N/mm for all tested ACLs. The stiffness showed only minor differences between the values for juvenile compared to adult ACL as well as for the three different test conditions (testing amplitudes 1.6 and 1.8 mm, testing velocities 5 and 20 mm/s; Figure 4(a)).

The toe-regions increased with higher testing velocity for all tested specimens (Figure 4(b)). The toe-region was almost twice as high for juvenile ACL compared to adult ACL for a test amplitude of 1.6 mm (5 mm/s: $(5.6 \pm 0.4)\%$ versus $(2.3 \pm 0.5)\%$; 20 mm/s: $(6.2 \pm 0.7)\%$ versus $(3.1 \pm 0.7)\%$). All tested ACLs exhibited a longer toe-region after the final hysteresis loop.

The energy dissipation decreased with an increasing testing velocity (from 5 to 20 mm/s) for all tested specimens from (2.078 ± 0.81) to (0.405 ± 0.28) mJ (Figure 5). A higher energy dissipation was observed at 1.8 mm amplitude for adult ACL (2.998 ± 0.46) mJ compared to juvenile ACL (0.484 ± 0.14) mJ. A similar trend was found when tested with an amplitude of 1.6 mm.

Embroidered scaffolds

Cyclic tensile testing. With test runs (A) and (B) the energy dissipation (ΔW) was determined to display the dependency of the strain (10% versus 20%) whereas with test runs (B) and (C) the influence of the testing velocity (5 versus 20 mm/s) shall be demonstrated. In order to compare scaffolds that were subjected to initial cyclic loading with the preloaded state, ΔW of the scaffolds was determined in (D) according to test run (A) (Figure 6).

(A) versus (B): The energy dissipation varied between (5.98 ± 1.66) mJ for P(LA-CL)-PDS and (11.88 ± 2.51) mJ for PLA-P(LA-CL) after the initial test run (A) and increased up to 400% with a doubled testing amplitude.

(B) versus (C): With increasing tensile testing velocity (from 5 to 20 mm/s), higher energy dissipation (up to 30%) was observed for all measured scaffolds. On the

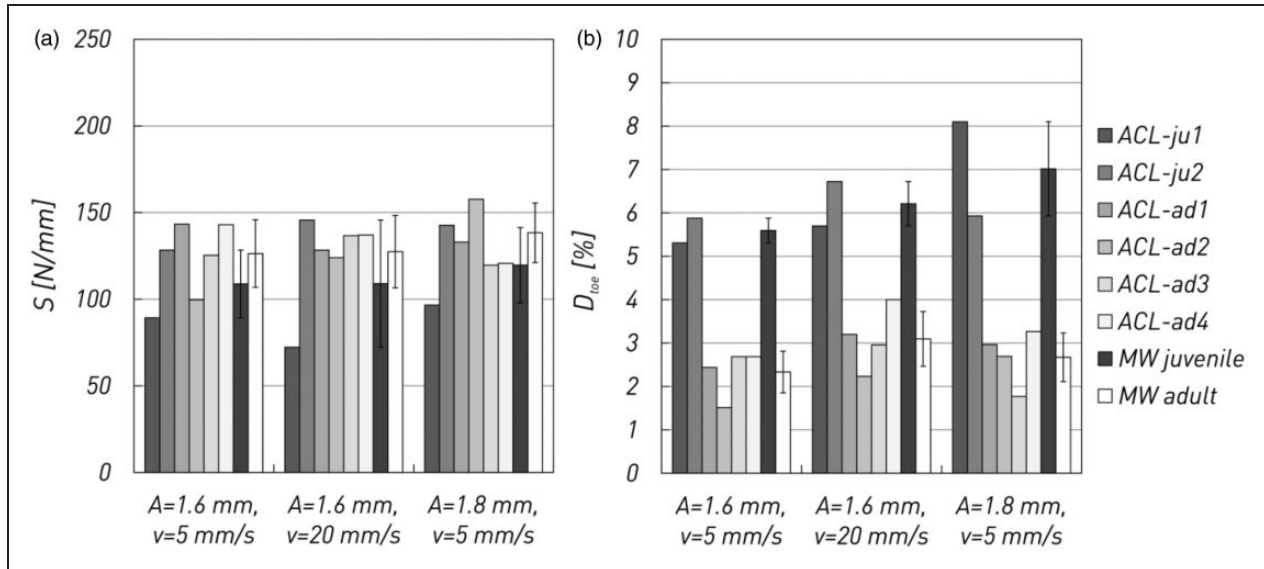


Figure 4. Mechanical parameters (a) stiffness (S) and (b) toe-region (D_{toe}) of native anterior cruciate ligament (ACL) for different testing amplitudes ($A = 1.6$ mm and $A = 1.8$ mm) and testing velocities ($v = 5$ mm/s and $v = 20$ mm/s).

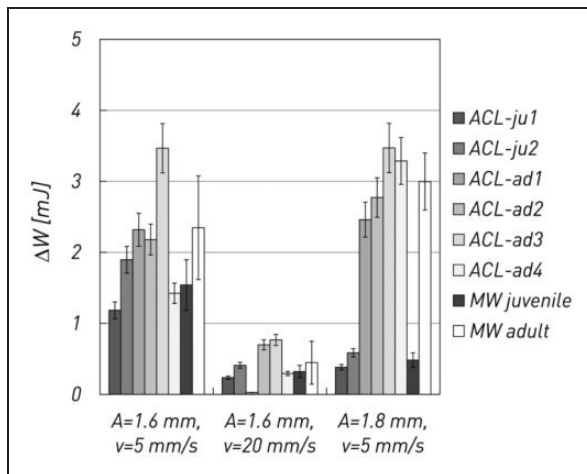


Figure 5. Energy dissipation (ΔW) of native anterior cruciate ligament (ACL) for different testing amplitudes ($A = 1.6$ mm and $A = 1.8$ mm) and testing velocities ($v = 5$ mm/s and $v = 20$ mm/s) under cyclic loading for five loops.

contrary, an increasing tensile testing velocity (from 5 to 20 mm/s) resulted in decreased energy dissipation values for the measured lapin native ACL tissue.

(A) versus (D): After the final test run ΔW decreased up to 31% for the majority of the tested scaffolds. However, PDS-PDS and P(LA-CL)-PDS showed increasing ΔW (15% and 29%, respectively).

All tested scaffolds with PLA as the thread material (upper or lower thread) exhibited lower values for the energy dissipation after cyclic loading. Energy dissipation of all tested scaffolds exceeded the values for native

ACL tissue (see Appendix 5 for exemplary comparison of hysteresis behavior for native ligament and embroidered scaffold).

Uniaxial tensile testing. The values for maximum tensile load (F_{max}) and maximum strain (ϵ_{max}) are specified in Table 2. Additional specification of the yield load [N] in Table 2 depends on the partial loss of structural function of embroidered scaffolds when the value is exceeded.

The highest maximum tensile load was determined for PDS-PLA-pre with (636.82 ± 40.77) N and a yield load of about 300 N. Scaffolds made of P(LA-CL)-P(LA-CL) offered the lowest maximum tensile load value with (186.13 ± 10.52) N and a yield load of about 60 N. The maximum strain was calculated with the lowest value for P(LA-CL)-P(LA-CL)-pre with (44.0 ± 0.5)% and the highest value for P(LA-CL)-PLA-un with (94.7 ± 3.2)%. Bi-component scaffolds made of PDS or P(LA-CL) as upper thread and PLA as lower thread exhibited higher maximum load values whether these scaffolds were unloaded or preloaded. The lower thread has to endure higher loads than the upper. No significant differences were identified between unloaded and preloaded scaffolds (the values for maximum tensile load and strain). However, tendencies indicated higher tensile load and lower strain values for preloaded scaffolds.

The stiffness was significantly higher for nearly all tested preloaded scaffolds after cyclic loading (Figure 7(a)). Highest stiffness value was determined for PLA-P(LA-CL)-pre with (249.53 ± 19.64) N/mm and PDS-P(LA-CL)-un with (47.48 ± 7.03) N/mm

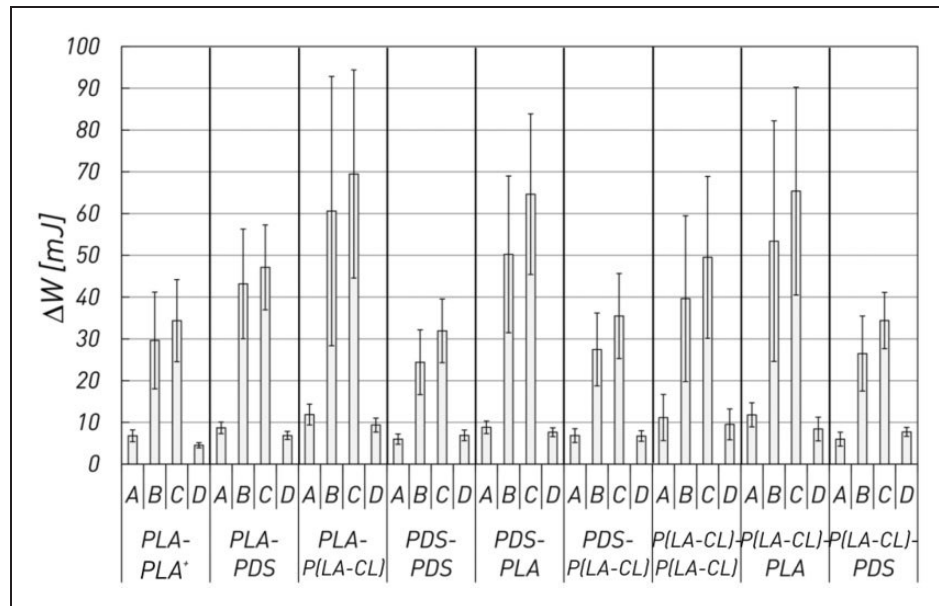


Figure 6. Energy dissipation (ΔW) of embroidered scaffolds made of different thread material combinations in upper and lower thread and tested under cyclic loading for ten loops and four different run settings: (A) 10% amplitude and 5 mm/s testing velocity; (B) 20% and 5 mm/s; (C) 20% and 20 mm/s; and (D) 10% and 5 mm/s. The first mentioned material identifies the upper thread and the second one the lower thread (e.g. poly(lactic acid-co- ϵ -caprolactone) (P(LA-CL))-polydioxanone (PDS)). *Only one layer for PLA-PLA.

referring to the lowest stiffness value. Bi-component scaffolds with PLA as thread material (upper or lower thread) exhibited higher stiffness values compared to bi-component scaffolds made of the monofilaments. The toe-region (Figure 7(b)) of the embroidered scaffolds varied between $(0.3 \pm 0.1)\%$ for PDS-P(LA-CL)-pre and $(2.0 \pm 0.1)\%$ at most for PDS-PLA-pre. Independent of the usage as upper or lower thread, scaffolds made of twisted multifilament PLA indicated a more distinct but not significantly higher toe-region compared to pure monofilament structures. The toe-region for PLA-scaffolds is comparable to toe-regions of tested adult ACL.

Discussion

The aim of this study was the evaluation of the mechanical properties of embroidered scaffolds made of different thread materials and configurations for the application as resorbable substrate for temporary ACL replacement. Therefore, a comparison with native lapine ACL was performed. The results of this study support the hypothesis that embroidered scaffolds exhibit adequate mechanical properties, which are comparable to the characteristics of native ligament tissue. In order to adapt key features, such as toe-region, stiffness and mechanical behavior under cyclic loading, the adjustment of the embroidery pattern and the careful selection of the thread materials are crucial points.

Native lapine ACLs were investigated in regard to their mechanical behavior under cyclic loading. Since the number of references in the field of hysteresis of ligament tissue is limited, the exemplary tests served the purpose of gaining reference data. Danto and Woo²⁸ investigated the mechanical properties of ACL compared to the patellar tendon at different strain rates of 0.003 mm/s (slow), 0.3 mm/s (medium) and 113 mm/s (fast). Significant differences in stiffness properties were not observed between the slow and medium strain rates. Only for large changes in the strain rate of more than two decades, significant differences in the stiffness, which were based on the viscoelasticity of ligament tissue, were found.

In addition, Lydon et al.³³ studied the failure properties of rabbit ACL at strain rates of 0.0001 m/s compared to 0.92 m/s (four decades). Significantly higher values of the maximum tensile load (202.4 N) and the stiffness (448.8 N/mm) were determined for the fast rate compared to the slow rate values of 116.8 N and 62.8 N/mm, respectively. This phenomenon may explain the results of this study indicating no differences between the values for toe-region and stiffness at testing velocities of 5 and 20 mm/s, which range in a similar dimension. Juvenile and adult ACLs showed a stiffness of (112.50 ± 37.54) and (130.69 ± 20.28) N/mm, respectively. These values are comparable to previously determined data for rabbit ACL.^{28,34}

Woo et al.³⁵ examined the tensile properties of rabbit medial collateral ligament at different ages. Younger

Table 2. Comparison of maximum tensile load (F_{\max}), maximum strain (ε_{\max}) and yield load of preloaded (pre) by cyclic tensile testing and unloaded (un) embroidered scaffolds. Scaffolds are made of three layers. Each layer consists of an upper and a lower thread (e.g. P(LA-CL)-PDS)

		F_{\max} [N]		ε_{\max} [%]		Yield load [N]
		mean	SD ^a	mean	SD	
PLA-PLA ^b	un	244.74	17.39	85.7	3.1	~100
	pre	242.72	12.89	76.1	8.1	~100
PLA-PDS	un	551.47	54.21	93.7	12.5	~280
	pre	572.08	49.36	83.4	6.3	~300
PLA-P(LA-CL)	un	539.57	35.37	82.2	3.4	~260
	pre	562.51	40.01	76.1	4.5	~260
PDS-PDS	un	296.54	47.27	61.4	7.9	
	pre	302.20	37.27	55.2	3.0	
PDS-PLA	un	631.89	47.74	93.7	7.1	~270
	pre	636.82	40.77	80.5	9.9	~300
PDS-P(LA-CL)	un	267.71	20.42	67.6	13.0	
	pre	285.78	33.65	53.2	7.0	
P(LA-CL)-P(LA-CL)	un	195.82	3.53	55.1	4.9	~60
	pre	186.13	10.52	44.0	0.5	~60
P(LA-CL)-PLA	un	558.56	31.89	94.7	3.2	~200
	pre	569.09	18.71	87.5	5.7	~220
P(LA-CL)-PDS	un	324.24	3.60	55.1	1.5	
	pre	332.51	10.86	54.4	1.0	

^a± Standard deviation.

^bOnly one layer.

P(LA-CL): poly(lactic acid-co- ε -caprolactone); PLA: poly(L-lactic acid); PDS: polydioxanone.

animals (age 1.5 months with body weight of 1500 g) with open epiphysis indicated lower stiffness and energy dissipation compared to animals at three months or older with a body weight of 3000 g. This is in agreement with the lower energy dissipation observed for juvenile ACL in this study. However, for the toe-region higher values were found for juvenile ACL compared to adult ACL. Possibly this is due to the fact that the ligament-to-bone transition with the typical enthesis and cartilage structure is fragmentary ossified at this age.³⁶ Higher toe-region values after the final hysteresis loop were determined for all tested ACLs. The cyclic loading causes micro cracks inside the ligament tissue and lower fiber waviness.³⁴ Due to the preloading, the ACL tissue has been extended, which is finally indicated by an increasing toe-region value. The energy dissipation decreases with an increasing testing velocity due to the viscoelasticity of ligament tissue reported by Viidik.³⁷

The transfer of the ACL characteristics to the scaffold properties is challenging, as material combination and scaffold structure are versatile factors and next to biomechanical aspects cell biological issues play an important role for tissue engineering concepts. Furthermore, the material degradation in vivo, altering the mechanical properties with time, has a crucial impact on the scaffold stability and durability. As a first step, the discussion of the mechanical properties of unaltered (dry state) scaffolds is part of this study only. The three utilized thread materials are controversial in terms of their applicability for the fabrication of resorbable scaffolds. The monofilaments PDS³⁸ and P(LA-CL)³⁹ are commercially available suture threads.

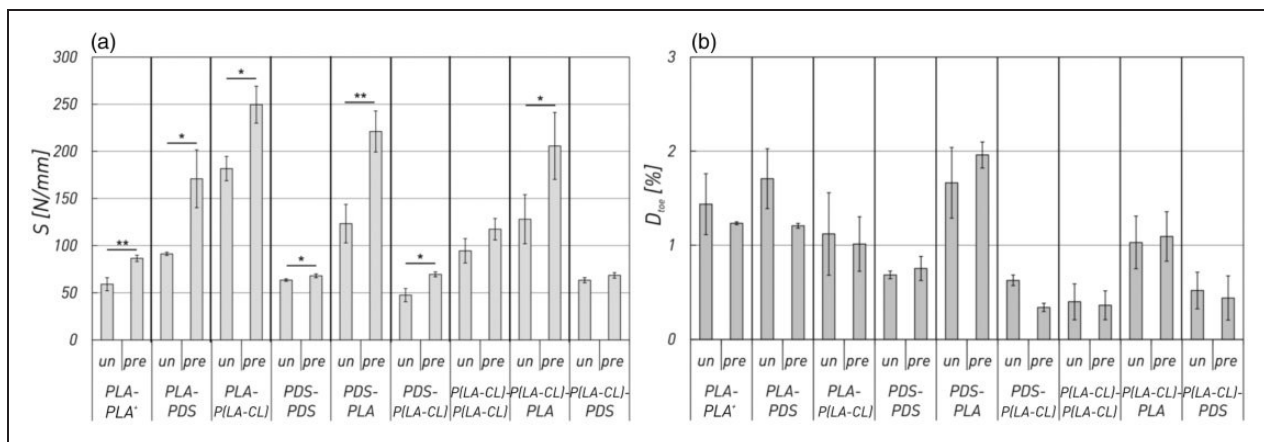


Figure 7. Mechanical parameters (a) stiffness (S) and (b) toe-region (D_{toe}) of unloaded (un) and preloaded (pre) embroidered scaffolds made of different thread material combinations in upper and lower thread. The first mentioned material identifies the upper thread and the second material the lower thread (e.g. poly(lactic acid-co- ε -caprolactone) (P(LA-CL))-polydioxanone (PDS)). *Only one layer for PLA-PLA; * $p < 0.05$ and ** $p < 0.005$ indicate significant differences.

PDS has been suggested as biomaterial for ACL reconstruction in the form of a reinforcement of an autologous transplant previously.^{40–42} The initial mechanical properties (maximum tensile load of 185 N) of a braided PDS scaffold were suitable for a tissue engineered lapin ligament substitute.⁴² However, the maximum tensile load decreased after six weeks in vivo by 42% due to the fast absorption. Therefore, it is unsuitable as single scaffold material.⁴² Scaffolds made of P(LA-CL) (copolymer of PLA and poly- ϵ -caprolactone (75:25 mol%)) indicated only low yield load and high strain. However, in vitro and in vivo studies with a surface-coated embroidered scaffold for bone grafts demonstrated the benefit for cell adherence and proliferation.^{43,44} As a reasonable compromise for embroidered ACL replacement structures P(LA-CL) can be used as the upper thread regarding the thread tension proportion in embroidered scaffolds (Appendix 1) and could therefore be more beneficial for cellular attachment. In combination with P(LA-CL) as the upper thread, the twisted PLA multifilament could be applied as the lower thread in the capacity of a mechanical stable material. The ratio of the upper thread to the lower thread is 2:1. Hence, the lower thread is placed more tautly and therefore extends first when taking up the initial agent load. Moreover, PLA was investigated as the upper and lower thread, indicating therefore proper mechanical properties for both positions. Lu et al.⁴⁵ analyzed braided scaffolds made of PLA or PLGA concerning primary ACL cell attachment, proliferation and the mechanical and degradation properties. Based on their results, PLA was a more suitable material for ACL reconstruction compared to PLGA.

Embroidery technology offers the possibility to produce textile scaffolds for medical applications with a predefined mechanical behavior. Compared to other textile technologies, the procedure of the pattern design facilitates the direct alignment of the thread material according to the requirements of the native tissue.²⁵ This results in an embroidered structure similar to the native fiber arrangement in ligament tissue shown by Viidik.³⁷ A scaffold pattern for ACL reconstruction was investigated and revealed adequate maximum tensile load and strain in the loading direction (Appendices 2–4). The maximum tensile load, measured under cyclic tensile testing, increased for all tested scaffolds when the strain was doubled or the testing velocity increased. It can be assumed that the structural bracing is caused by cyclic loading, especially due to the contraction of the thread loops in the embroidered structure. This is supported by the fact that a higher stiffness was exhibited for preloaded scaffolds compared to unloaded scaffolds (Figure 7(a)). Hence, the results suggest that the viscoelastic behavior of the embroidered scaffolds is comparable to that of

native tissue. Moreover, the energy dissipation of the embroidered scaffolds exceeded, after the first loading cycle, the values of native ACL tenfold. However, the following cyclic loading effects the energy dissipation in such a way that it decreases. The use of preloaded scaffolds for in vitro experiments seems reasonable based on the structural hardening and the decreased energy dissipation after cyclic loading. Embroidered scaffolds made of PDS-PLA or P(LA-CL)-PLA demonstrated yield load values between 250 and 300 N and yield strain values between 18% and 20%, respectively. The maximum tensile load of a monofilament scaffold made of P(LA-CL)-PDS is equal to the yield load of PDS-PLA or P(LA-CL)-PLA. However, the maximum strain value of a P(LA-CL)-PDS scaffold is twice as high as for lapine ACL.⁴⁶ Furthermore, the embroidered scaffolds made of either of the monofilaments (P(LA-CL) or PDS) only exhibited an insufficient toe-region. Freeman et al.¹⁸ investigated the mechanical properties of braid-twist scaffolds made of PLA for the tissue engineering of ACL. The use of twisted PLA multifilament resulted in a distinctive toe-region, which is comparable to native ligament tissue. Here, a similar twisted multifilament made of PLA was applied and showed an increased toe-region compared to scaffolds made of monofilaments. Among beneficial mechanical properties (e.g. smaller diameter results in appreciable change in the flexibility), the introduced melt spun PLA multifilament implicates the possibility to adapt the yarn characteristic in the diameter dimension and mechanical behavior by modifying the manufacturing process compared to commercially available suture threads, which are limited in dimension and therefore also limited in flexibility and related tensile properties.

Embroidery technology offers the possibility to influence all of the above-mentioned parts of the load-strain behavior by using different thread materials as upper and lower thread (Figure 8). The presented mechanical properties of embroidered scaffolds made of PDS-PLA or P(LA-CL)-PLA are similar to the mechanical characteristics of native lapine ACL, reported elsewhere, with maximum tensile load values between 218 and 402 N and maximum strain values between 22% and 40%.^{29,33,47–49} Furthermore, Hoyer et al.²⁷ demonstrated that these embroidered polymer-hybrid scaffolds with an integrated collagen foam are potential substrates for the ACL reconstruction. Hence, the ongoing study focuses on in vitro and in vivo experiments to investigate mechanostimulated cell attachment and proliferation, the mechanical behavior under hydrolysis and in vivo degradation. Moreover, the next approaches will include the adjustment of the PLA multifilament thread and the development of an embroidered scaffold with three different structure

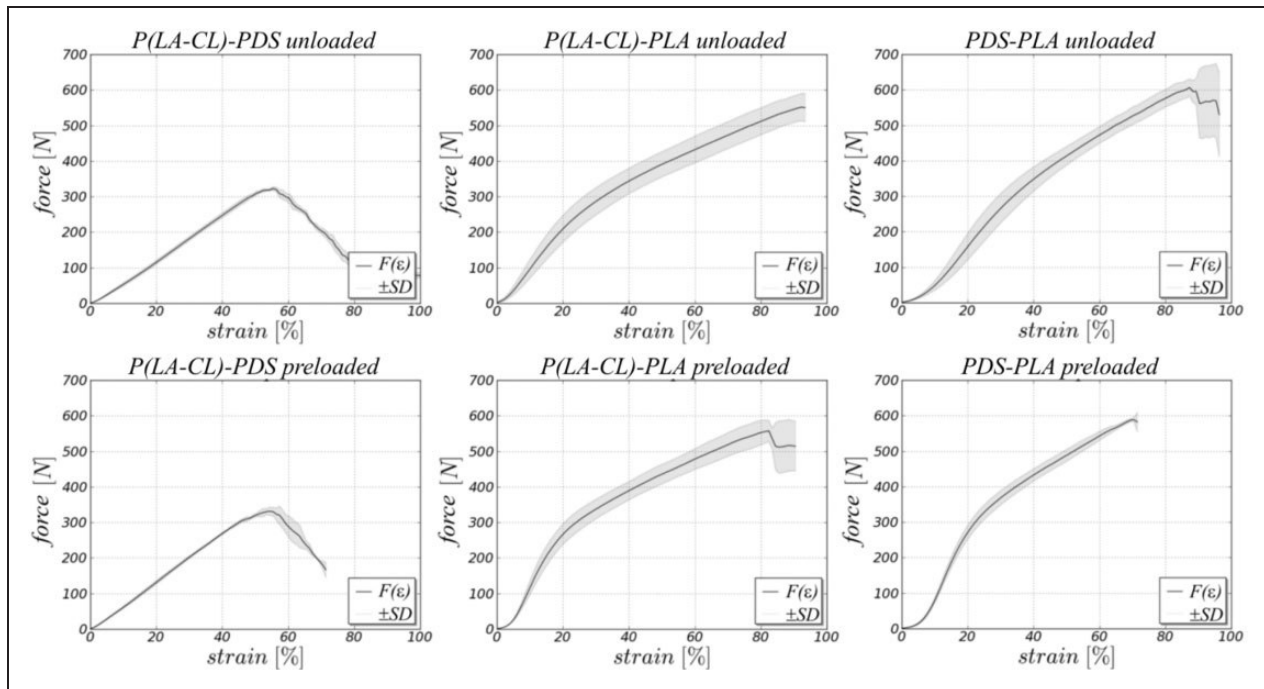


Figure 8. Comparison of the load–strain behavior ($F(\epsilon) \pm SD$, mean \pm standard deviation) of different unloaded and preloaded embroidered scaffolds (poly(lactic acid-co- ϵ -caprolactone) (P(LA-CL))-polydioxanone (PDS), P(LA-CL)-poly(L-lactic acid) (PLA), PDS-PLA).

zones (ligament, enthesis and osteochondral part) according to the constitution of native ACL by a mimicked pattern design.

Conclusion

The mechanical behavior of embroidered scaffolds, made of PLA, PDS and P(LA-CL) threads or combinations of them, was investigated by means of tensile testing and cyclic loading tests. In addition, exemplary studies with native lapine ACL were analyzed to characterize the hysteresis behavior and typical mechanical parameters. According to the used thread material and the used embroidery pattern, embroidered scaffolds presented in this study were tailored to possess an adaptable viscoelastic behavior, a sufficient toe-region and similar values for the maximum tensile load and strain comparable to the mechanical properties of lapine ACL.

Funding

This work was supported by the Deutsche Forschungsgemeinschaft [HE 4466/22-1].

Acknowledgments

The authors acknowledge Nicole Schneider for scaffold preparation, Lars Bittrich for programming the Python code to evaluate lapine ACL data and Holger Scheibner (all IPF

Dresden) for providing assistance with cyclic tensile testing the embroidered scaffolds within this project.

References

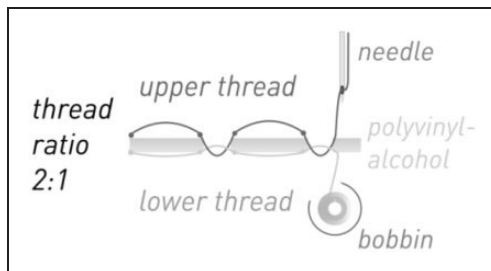
- Nicholl JP, Coleman P, Williams BT, et al. Injuries in sport and exercise: main report. Sports Council, 1993.
- Woo SL-Y, Abramowitch SD, Kilger R, et al. Biomechanics of knee ligaments: injury, healing, and repair. *J Biomech* 2006; 39: 1–20.
- Woo S-Y, Smith BA, Livesay GA, et al. (i) Why do ligaments fail? *Curr Orthop* 1993; 7: 73–84.
- Bollen S. Epidemiology of knee injuries: diagnosis and triage. *Br J Sports Med* 2000; 34: 227–228.
- Murray MM, Vavken P and Fleming B. *The ACL handbook: Knee biology, mechanics, and treatment*, 1st ed. Dordrecht: Springer, 2013.
- Wilcke A. *Vordere Kreuzbandläsion: Anatomie, Pathophysiologie, Diagnose, Therapie, Trainingslehre, Rehabilitation; mit 106 Tabellen*. Darmstadt: Steinkopff, 2004.
- Stringham DR, Pelmas CJ, Burks RT, et al. Comparison of anterior cruciate ligament reconstructions using patellar tendon autograft or allograft. *Arthrosc J Arthrosc Relat Surg* 1996; 12: 414–421.
- Kartus J, Movin T and Karlsson J. Donor-site morbidity and anterior knee problems after anterior cruciate ligament reconstruction using autografts. *Arthrosc J Arthrosc Relat Surg* 2001; 17: 971–980.
- Laurencin CT and Freeman JW. Ligament tissue engineering: an evolutionary materials science approach. *Biomaterials* 2005; 26: 7530–7536.

10. Dandy DJ and Gray AJ. Anterior cruciate ligament reconstruction with the Leeds-Keio prosthesis plus extra-articular tenodesis. Results after six years. *J Bone Joint Surg* 1994; 76: 193–197.
11. Ghalayini SRA, Helm AT, Bonshahi AY, et al. Arthroscopic anterior cruciate ligament surgery: Results of autogenous patellar tendon graft versus the Leeds-Keio synthetic graft. *Knee* 2010; 17: 334–339.
12. Kuo CK, Marturano JE and Tuan RS. Novel strategies in tendon and ligament tissue engineering: advanced biomaterials and regeneration motifs. *Sports Med Arthrosc Rehabil Ther Tech* 2010; 2: 20.
13. Vunjak-Novakovic G, Altman G, Horan R, et al. Tissue engineering of ligaments. *Annu Rev Biomed Eng* 2004; 6: 131–156.
14. Gupta BS. Medical textile structures: an overview. *Medical Plastics and Biomaterials Magazine* 1998; 5: 16–30.
15. Ratner BD. *Biomaterials science: An introduction to materials in medicine*. Amsterdam, Heidelberg: Elsevier, Academic Press, 2012.
16. Cooper JA, Lu HH, Ko FK, et al. Fiber-based tissue-engineered scaffold for ligament replacement: design considerations and in vitro evaluation. *Biomaterials* 2005; 26: 1523–1532.
17. Fan H, Liu H, Toh SL, et al. Anterior cruciate ligament regeneration using mesenchymal stem cells and silk scaffold in large animal model. *Biomaterials* 2009; 30: 4967–4977.
18. Freeman JW, Woods MD and Laurencin CT. Tissue engineering of the anterior cruciate ligament using a braid-twist scaffold design. *J Biomech* 2007; 40: 2029–2036.
19. Laurent CP, Ganghoffer J-F, Babin J, et al. Morphological characterization of a novel scaffold for ACL tissue engineering. *J Biomech Eng* 2011; 133: 1–9.
20. Walters VI, Kwansa AL and Freeman JW. Design and analysis of braid-twist collagen scaffolds. *Connect Tissue Res* 2012; 53: 255–266.
21. Sahoo S, Cho-Hong JG and Siew-Lok T. Development of hybrid polymer scaffolds for potential applications in ligament and tendon tissue engineering. *Biomed Mater* 2007; 2: 169–173.
22. Ellis JG. *Engineering and surgical textiles by embroidery*. Presentation on Textile Institute 80th World Conference, Manchester, 2000.
23. Karamuk E, Mayer J and Wintermantel E. Sticktechnologie für medizinische Textilien und Tissue Engineering. In: Wintermantel E and Ha S-W (eds) *Medizintechnik*. Springer: Berlin, Heidelberg, 2009, pp.951–960.
24. Warrior NA, Rudd CD and Gardner SP. Experimental studies of embroidery for the local reinforcement of composites structures: 1. Stress concentrations. *Compos Sci Technol* 1999; 59: 2125–2137.
25. Gliesche K, Breier A and Schmack G. Herstellung textiler Scaffolds mittels Sticktechnik. *BIOMaterialien* 2005; 6: 155–159.
26. Rentsch C, Schneiders W, Hess R, et al. Healing properties of surface-coated polycaprolactone-co-lactide scaffolds: a pilot study in sheep. *J Biomater Appl* 2013; 28: 654–666.
27. Hoyer M, Drechsel N, Meyer M, et al. Embroidered polymer–collagen hybrid scaffold variants for ligament tissue engineering. *Mater Sci Eng C* 2014; 43: 290–299.
28. Danto MI and Woo SL-Y. The mechanical properties of skeletally mature rabbit anterior cruciate ligament and patellar tendon over a range of strain rates. *J Orthop Res* 1993; 11: 58–67.
29. Panjabi MM and Courtney TW. High-speed subfailure stretch of rabbit anterior cruciate ligament: changes in elastic, failure and viscoelastic characteristics. *Clin Biomech* 2001; 16: 334–340.
30. Takeda Y, Xerogeanes JW, Livesay GA, et al. Biomechanical function of the human anterior cruciate ligament. *Arthrosc J Arthrosc Relat Surg* 1994; 10: 140–147.
31. Karmani S and Ember T. The anterior cruciate ligament - I. *Curr Orthop* 2003; 17: 369–377.
32. Böl M, Leichsenring K, Weichert C, et al. Three-dimensional surface geometries of the rabbit soleus muscle during contraction: input for biomechanical modelling and its validation. *Biomech Model Mechanobiol* 2013; 12: 1205–1220.
33. Lydon C, Crisco J, Panjabi M, et al. Effect of elongation rate on the failure properties of the rabbit anterior cruciate ligament. *Clin Biomech* 1995; 10: 428–433.
34. Sekiguchi H, Han J, Ryu J, et al. The characterization of mechanical properties of a rabbit femur-anterior cruciate ligament-tibia complex during cyclic loading. *J Jpn Soc Mech Eng* 2001; 44: 276–281.
35. Woo SL-Y, Orlando CA, Gomez MA, et al. Tensile properties of the medial collateral ligament as a function of age. *J Orthop Res* 1986; 4: 133–141.
36. Schneider H. Zur Struktur der Sehnenansatzzonen. *Anat Embryol* 1956; 119: 431–456.
37. Viidik A. Biomechanical behavior of soft connective tissue. In: *proceedings of the NATO Advanced Study Institute on progress in biomechanics* (ed A Nuri), Ankara, Turkey, 10–21 July 1978, pp.75–113. Alphen aan den Rijn: Sijthoff & Noordhoff [International Publishers], 1979.
38. Ray JA, Doddi N, Regula D, et al. Polydioxanone (PDS), a novel monofilament synthetic absorbable suture. *Surg Gynecol Obstet* 1981; 153: 497–507.
39. Tomihata K, Suzuki M, Oka T, et al. A new resorbable monofilament suture. *Polymer Degrad Stabil* 1998; 59: 13–18.
40. Häfner M. *Die augmentierte Kreuzbandnaht*. Dissertation, LMU München: Tierärztliche Fakultät, 2004.
41. Puddu G, Cipolla M, Cerullo G, et al. ACL reconstruction and augmentation with PDS graft. *Clin Sports Med* 1993; 12: 13–24.
42. Rehm KE and Schultheis KH. Transposition of ligaments with polydioxanone (PDS®). *Unfallchirurgie* 1985; 11: 264–273.
43. Rentsch B, Bernhardt R, Scharnweber D, et al. Embroidered and surface coated polycaprolactone-co-lactide scaffolds: a potential graft for bone tissue engineering. *Biomater* 2012; 2: 158–165.
44. Rentsch B, Hofmann A, Breier A, et al. Embroidered and surface modified polycaprolactone-co-lactide scaffolds as bone substitute: in vitro characterization. *Ann Biomed Eng* 2009; 37: 2118–2128.
45. Lu HH, Cooper JA, Manuel S, et al. Anterior cruciate ligament regeneration using braided biodegradable

- scaffolds: in vitro optimization studies. *Biomaterials* 2005; 26: 4805–4816.
46. Woo SL, Newton PO, MacKenna DA, et al. A comparative evaluation of the mechanical properties of the rabbit medial collateral and anterior cruciate ligaments. *J Biomech* 1992; 25: 377–386.
47. Azangwe G, Mathias KJ and Marshall D. The effect of torsion on the appearance of the rupture surface of the ACL of rabbits. *Knee* 2002; 9: 31–39.
48. Azangwe G, Mathias KJ and Marshall D. Preliminary comparison of the rupture of human and rabbit anterior cruciate ligaments. *Clin Biomech* 2001; 16: 913–917.
49. Hefti FL, Kress A, Fasel J, et al. Healing of the transected anterior cruciate ligament in the rabbit. *J Bone Joint Surg* 1991; 73: 373–383.

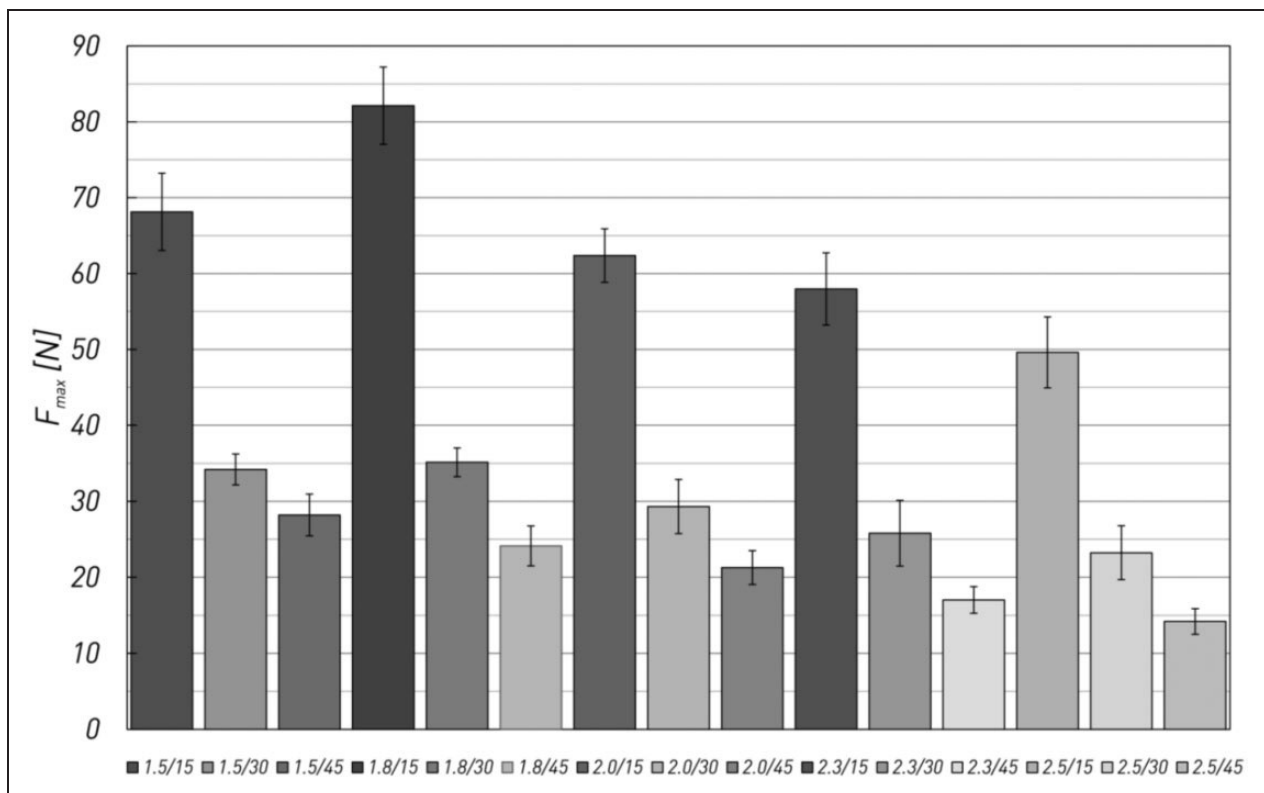
Appendix I

Assembly of the thread materials in an embroidered structure.



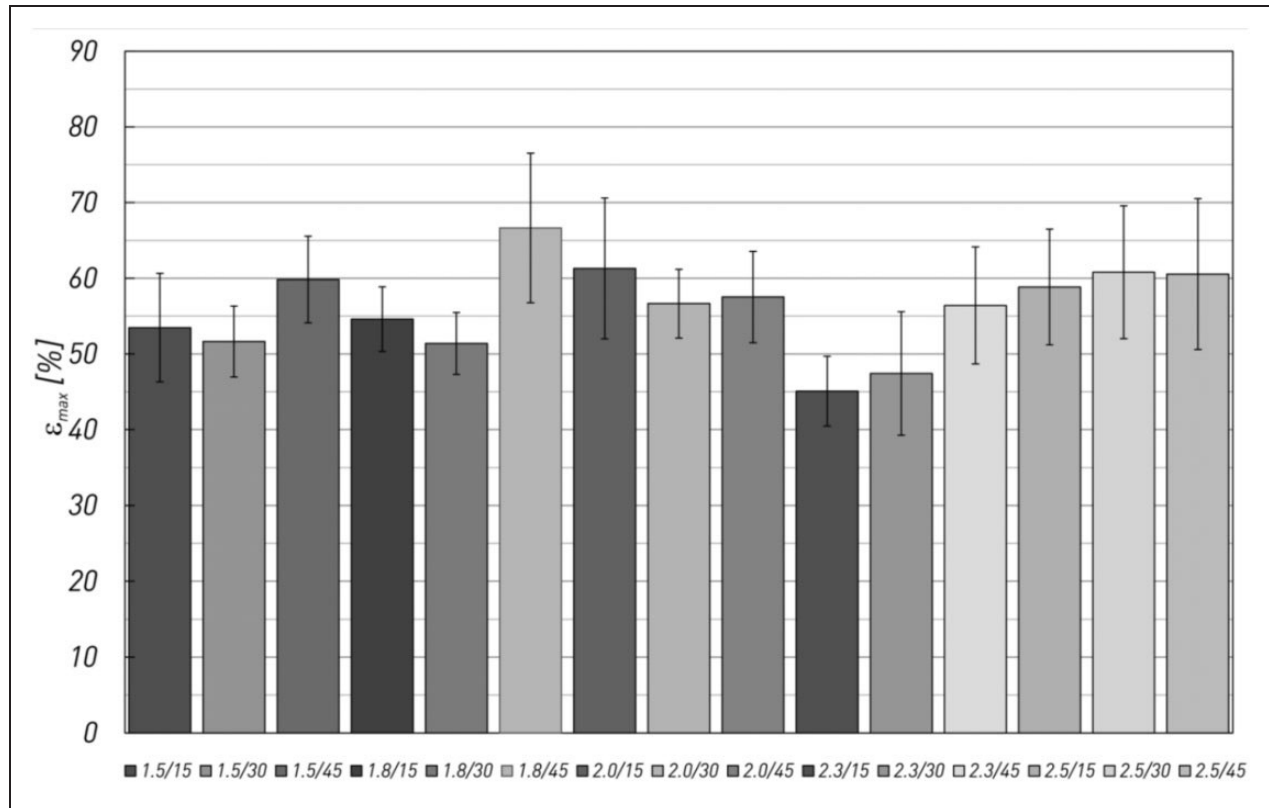
Appendix 2

Maximum tensile load (F_{\max}) of the embroidery pattern (e.g. 1.8/45 pattern with 1.8 mm stitch length and 45° stitch angle) with different stitch lengths (1.5, 1.8, 2.0, 2.3 and 2.5 mm) and stitch angles (15°, 30°, 45°) of one-layer samples. Embroidery pattern 1.8/15 showed the highest tensile load value.



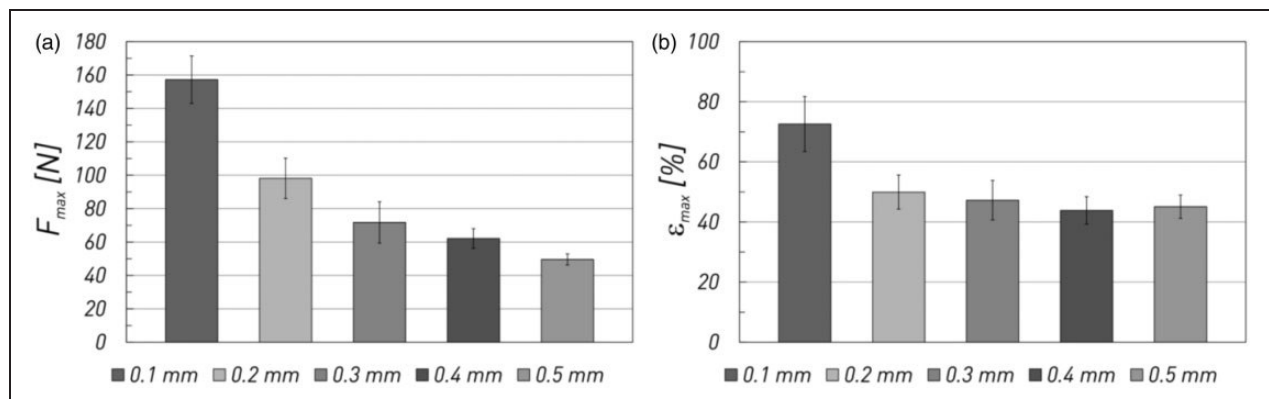
Appendix 3

Maximum strain (ϵ_{\max}) of the embroidery pattern (e.g. 1.8/45 pattern with 1.8 mm stitch length and 45° stitch angle) with different stitch lengths (1.5, 1.8, 2.0, 2.3 and 2.5 mm) and stitch angles (15°, 30°, 45°) of one-layer samples. No significant differences were evaluated between strain values of the tested embroidery pattern.



Appendix 4

(a) Maximum tensile load (F_{\max}) and (b) maximum strain (ϵ_{\max}) of the embroidery pattern 1.8/15 with different duplication shifts (0.1, 0.2, 0.3, 0.4 and 0.5 mm) of one-layer samples. An optimal duplication shift was achieved for 0.2 mm due to the low strain value and the high tensile load value.



Appendix 5

Exemplary mechanical behavior (energy dissipation as gray dyed area) under similar cyclic tensile testing conditions of $\sim 20\%$ strain and 5 mm/s testing velocity for (a) lapine ACL tissue and (b) an embroidered scaffold made of PLA-PDS.

